



**Beyond the Specifications for O-rings - Using Good Science to Answer the Form,
Fit and Function Questions**

Robert W. Keller
Simrit
A Division of Freudenberg-NOK

Presented at the Fall 174th Technical Meeting of the
Rubber Division of the American Chemical Society, Inc.
Louisville, KY
October 14-16, 2008

ISSN: 1547-1977

Abstract

Particularly in many aerospace applications, the customer and supplier of an O-ring rely on the part drawing and associated materials specification to make decisions about whether the O-ring is appropriate for an application. That all works well, many times, but there are many instances where the O-ring is supplied to all the documented requirements yet still leaks or fails in the application. Aerospace application failures tend to invite a lot more attention than automotive application failures since aerospace O-ring failures usually involve leakage and grounded aircraft or worse. In this paper, application examples and case histories will be used to demonstrate the utility of several scientific techniques (gland analyses and installation analyses, testing at application temperatures in application fluids, FEA analyses, and simulated functional tests) will be used to illustrate problem solving in these demanding applications. In many cases, we need to go much farther than just the part print and material specification to truly analyze Form, Fit and Function of an O-ring.

Beyond the Specifications for O-rings - Using Good Science to Answer the Form, Fit and Function Questions

Introduction

In general, most believe that the form, fit and function of O-rings should be a relatively straightforward subject. There are excellent industry standard specifications for O-ring size, quality requirements and material requirements and O-ring manufacturers generally publish design guides which help the end user specify the proper O-ring as well as design the mating gland. In a perfect world, that would be the end of the story. However, it's not a perfect world and many O-rings are manufactured to non-standard sizes and for non-standard mating glands. Also, performance of the O-ring material at application temperatures and pressures is not truly defined in many of the material specifications. This paper gives examples of Fit and Function that are not straightforward to analyze without thorough material models and Finite Element Analyses. In other words, the specifications for the rubber material and the gland will not provide the Fit and Function answers.

In most cases, elastomer materials for sealing applications are developed around existing or target specifications. Examples of such specifications are the ASTM D2000¹ material callouts and the AMS industry specifications for aerospace materials published by SAE International. These specifications will generally define the basic mechanical properties needed along with some time dependent

properties such as thermal air aging, resistance to application fluids, or compression set resistance. Generally, these specifications do a pretty good job of defining the materials that will be suitable for an application. However, these specifications will not help answer the question of how a rubber seal material will behave at application temperatures under application pressures. This paper will cover a couple of examples where FEA can be used to further define the suitability of the material for the application and to troubleshoot application problems. The advantage of FEA calculations is that they can be done without the expense of building test fixtures or the expense of building up components and evaluating the seals in the field. Sometimes, building up components and evaluating seals in the field is just too risky, as in the case of jet engine fuel controls - it is doubtful that passengers would be amenable to flying on an airliner with "experimental" fuel control assemblies.

Traditionally, one of the issues with FEA analysis of rubber sealing systems is that rubber is a non-linear material. This has meant phenomenological models to curve fit stress-strain properties and iterative computer solutions. Until the development of very powerful desktop computer processors, these iterative calculations were rather expensive to do on the few super computers available. With current computer processor technologies, these iterative calculations have become fairly inexpensive to generate.

The key to getting fairly accurate models of rubber behavior has been in modeling the non-linear character of rubber materials. A linear elastic material simply follows a direct proportionality between stress and strain.

$$\sigma = k\gamma \quad [1]$$

Where, σ = stress

γ = strain.

The general strain energy function for non-linear, hyper elastic materials such as rubber is in the form of Equation [2]²:

$$W = \sum_{i,j=0}^{M,N} C_{ij}(I_1 - 3)^i (I_2 - 3)^j \quad [2]$$

Where, W = Strain energy function

C_{ij} = empirically determined material parameters (curve fitting)

$I_1, I_2, \text{ etc.}$ = strain invariants.

Infinite series, such as Equation [2] are not at all practical for general use. The first approximation of material behavior is the Mooney-Rivlin model which has been used extensively in analysis of rubber elasticity^{2, 3, 4, 5} :

$$W = C_{10}(I_1 - 3) + C_{01}(I_2 - 3) \quad [3]$$

or for uniaxial tension:

$$\sigma_{11} = 2C_{10}(\lambda^2 - (1/\lambda)) + 2C_{01}(\lambda - (1/\lambda^2)) \quad [4]$$

where, σ_{11} = true stress in the primary direction of strain

λ = extension ratio (L/L_0) of the test piece

C_{10} and C_{01} are determined from curve fitting of true stress versus extension ratio per equation [4].

While equation [4] does a pretty good job of describing stress-strain behavior at low strains, it deviates from the observed behavior at higher strains. These higher strains are often of more interest in pressure applications of seals since we are concerned with how the material behaves at the extrusion gap under high strains. A longer series is thus needed to define material behavior at higher strains.

The Ogden model is often used to better describe the behavior of rubber materials at higher strains⁶:

$$U = \sum_{i=1}^N (2\mu_i / \alpha_i^2) (\lambda_1^{\alpha_i} + \lambda_2^{\alpha_i} + \lambda_3^{\alpha_i} - 3) + \sum_{i=1}^N (1/D_i) (J^{el} - 1)^{2i} \quad [5]$$

where, U = strain energy potential

N = order of polynomial = 1 to 3 in most cases

$\lambda_1, \lambda_2,$ and λ_3 = the three principal stretches

$\mu_i, \alpha_i,$ and D_i are temperature dependent material properties defined from curve fitting.

For uniaxial tension, the Ogden model becomes:

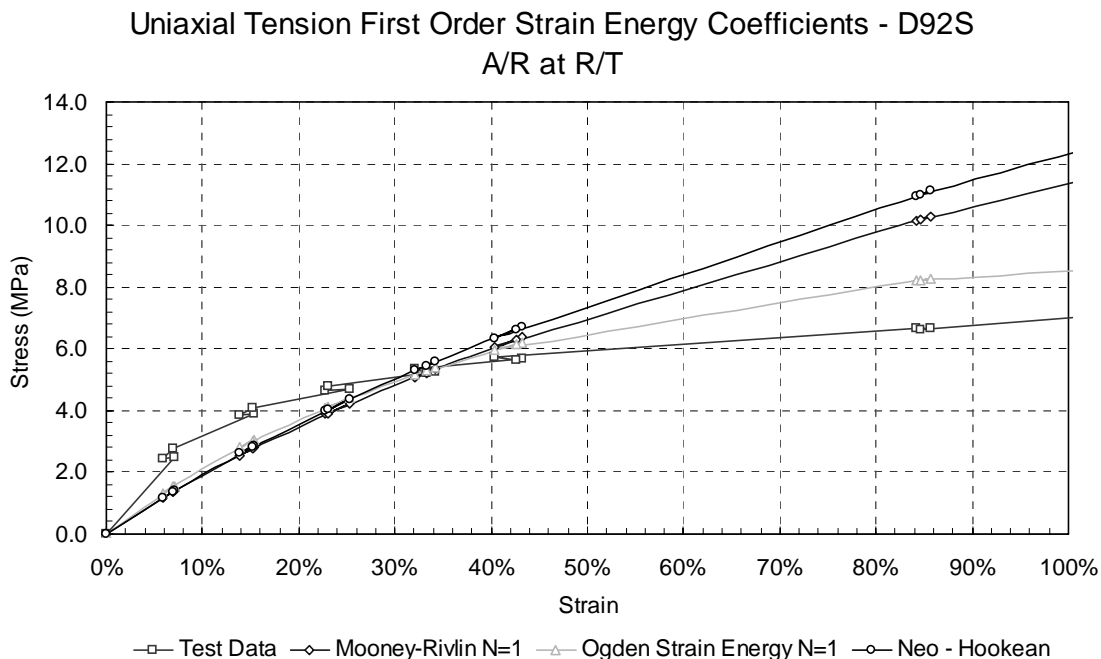
$$\sigma_{11} = \sum_{i=1}^r \beta_i (\lambda^{\alpha_i} - \lambda^{-\alpha_i/2}) \quad [6].$$

None of these models does a great job of describing the stress-strain properties of filled elastomers used in commercial applications. Abaqus software has recently introduced the Marlow model which simply fits the curves generated in stress and strain

for the elastomer sample of interest. With the pressures typically encountered with O-rings in Aerospace and industrial applications, the elastomer can be regarded as incompressible and sufficient data from uniaxial stress-strain measurements can be used to predict planar and shear stress situations. While some may find this to be an over-simplification without having biaxial and bulk modulus data, we have found that using the uniaxial data alone is sufficient to predict the behavior of elastomers in the application as the reader will find in later sections of this paper. This Marlow curve fitting model is used in our material property analyses and FEA modeling.

Typical comparison of actual test data with the Mooney-Rivlin and Ogden models is shown in Figure 1.

Figure 1



Refinement of the Ogden model can be achieved by increasing the order of the Ogden series. However, this still does not truly fit the model to the experimental data as shown in Figure 2.

Figure 2

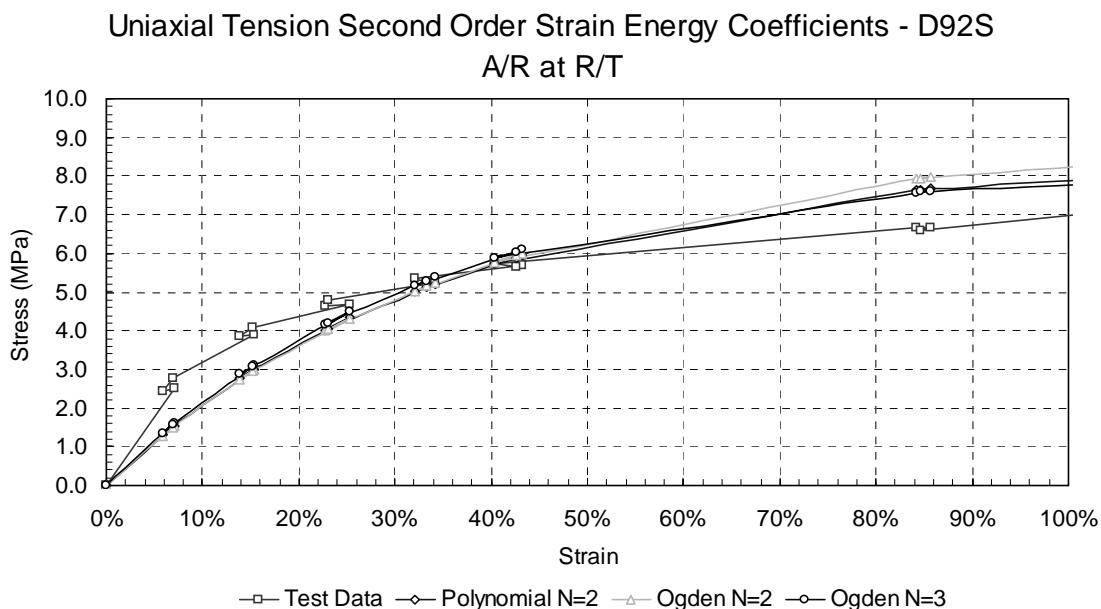
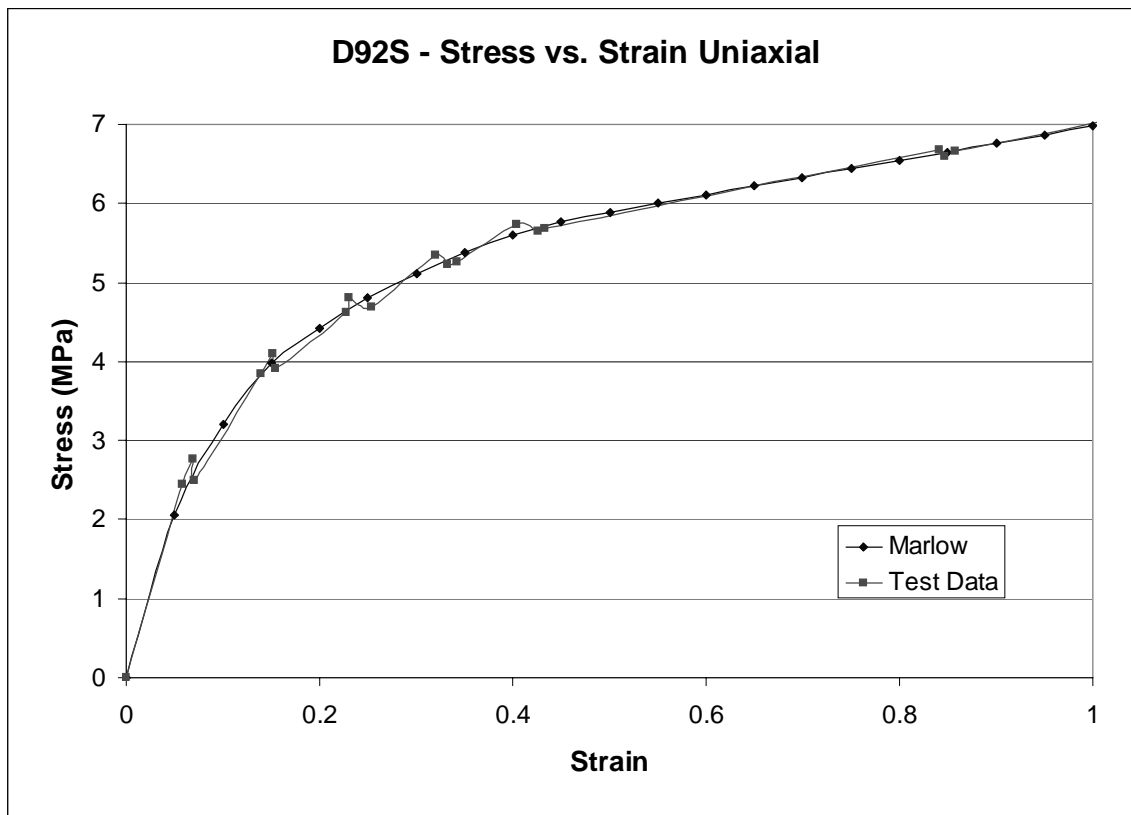


Figure 3 shows the fit using the Marlow curve fitting model and the excellent agreement between the experimental data and the model.

Figure 3



Experimental

Development of material model parameters was done at desired temperature using a tensile stress-strain tester with a temperature controlled box capable of maintaining specimen temperatures in the range of -70°C to $+250^{\circ}\text{C}$. Testing was done on ASTM D412 die C tensile test specimens with optical extension measurements. The Marlow curve fitting model was then used in the iterative calculations of the O-rings in the application under pressure.

Our generation of stress-strain data is designed to give an equilibrium value of stress at a given strain. Thus, we extend the sample to the desired strain, usually in 0.05 strain intervals (5% elongation intervals), cycle the specimen around the desired strain

point to get rid of the Mullins stress-softening effect, and then hold at the desired strain for 3 minutes to give the bulk of the stress relaxation. This process is repeated at each desired strain (elongation) value until specimen break. By doing the testing in this way, we alleviate the initial high stress at a given strain (Mullins effect) and approximate equilibrium stress relaxation at the target strain. This simulates a material that is fully stress-softened and relaxed at the target strain. Simple stress-strain extension experiments at a set cross-head rate do not give the fully stress-softened and relaxed curves for the material. Triplicate testing is done to assure test consistency.

The test temperatures and pre-soak conditions for the materials were provided by the end application customers for the O-rings.

A case of improper Fit

As mentioned in the introduction, there are many non-standard O-rings and many non-standard glands used in the actual application. In most of these cases, the non-standard situations cannot be analyzed by canned O-ring software. I will discuss a particular situation here where a very small O-ring was used to seal the interface between a reinforced plastic housing and a metal tube going into the housing assembly. The customer noted sporadic high installation forces and sporadic fracture of the reinforced plastic housing. A cross-sectional view of this assembly is shown in Figure 4. The only way to "see" the problem was to perform material

property evaluations and model the progression of the assembly to look at loads and forces. The results of these analyses are shown in Table 1 and Figure 5. Essentially, at certain conditions, the O-ring would approach overflow of the resulting gland creating huge jumps in installation loads and potential for rupture of the mating reinforced plastic housing. The solutions were to modify the design and assembly to eliminate the possibility of O-ring overflow.

Figure 4

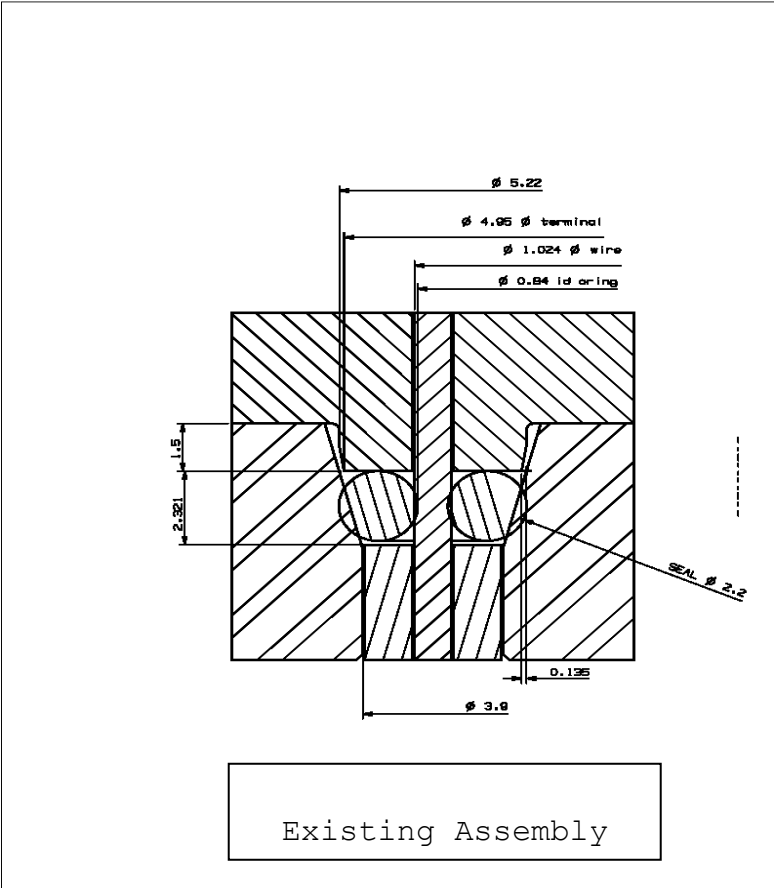
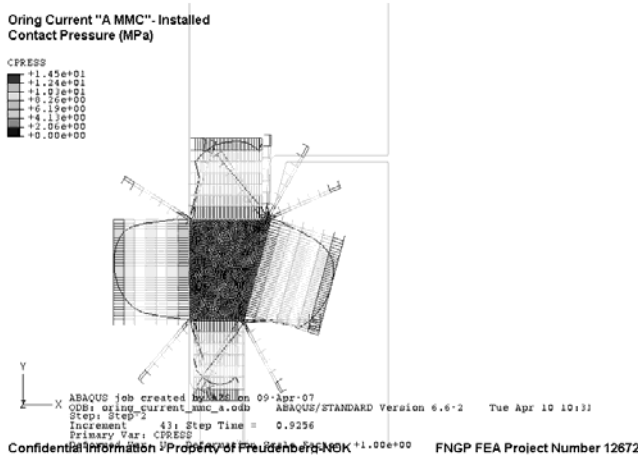


Table 1

FEA Matrix 1 Results			
Model #	Radial Load (N)	Axial Force (N)	Comments
1	10.05	32.38	Minimum squeeze
2	61.34	176.05	Nominal squeeze
3	94.75	235.04	Maximum squeeze
4	23.17	55.78	O-ring ID max
5	68.87	187.45	O-ring OD max
6	63.35	168.62	O-ring ID & OD max
7	74.02	210.82	Wire dia max
8	38.47	113.91	Bore Taper Angle max

Figure 5 - note the over-fill condition created excessive contact pressures

**Maximum Installed Condition
– Contact Pressure**



Function Case I results - High pressure, high temperature jet fuel application

In this case, the desired outcome of the development program was a material that would accommodate both high and low temperature extremes for a pressurized fuel control application. Traditionally, Fluorosilicone (FVMQ) materials had been used in these applications

due to their excellent low temperature flexibility. Recent developments by the polymer manufacturers of Fluorocarbon (FKM) materials had produced polymers with glass transition temperatures (Tg) of -40°C or slightly lower. These FKM materials were believed to be tougher and more pressure resistant than the relatively fragile FVMQ materials for installation and for resistance to pressure. The testing and the FEA analyses were done to understand whether a rubber compound based on one of these new low temperature polymers would work in the customer's application.

The key behaviors of the material for this fuel application were defined by conventional mechanical testing and by immersion and compression set testing. The behaviors of the materials used in this testing are summarized in Tables 2-5 for three FKM type materials and an FVMQ material used as a reference. A brief summary of the materials used is as follows:

1. FKM V75 - AMS7276 compliant and QPL'd material - standard bisphenol cured copolymer FKM with a Tg of roughly -20°C of 66 mole percent fluorine polymer, carbon black filled, 75 nominal Shore A hardness
2. FKM V115 - AMS-R-83485 compliant and QPL'd material - peroxide cured terpolymer with a Tg of -30°C of 65 mole percent fluorine polymer, carbon black filled, 75 nominal Shore A hardness

3. FKM V127 - peroxide cured terpolymer with a Tg of -42°C of 69 mole percent fluorine polymer, carbon black filled, 75 nominal Shore A hardness
4. FVMQ F80 - MIL-R-25988 Class 1 Grade 80 compliant material, Tg of -80°C , Silica filled, blue color

Using the customer's most demanding application for O-rings in terms of tolerance stacks and extrusion clearances, the material testing was done at 23°C and at 150°C where the extremes of the application were expected. This material testing was done as described in the Experimental section to give fully stress-softened and relaxed properties of the rubber material. These material properties were used in a Marlow curve fitting model to generate the material coefficients used in the iterative calculations for the FEA model. The FEA model of the O-ring assembled in the gland was then used with the anticipated extremes of pressure provided by the customer. The critical factor in this analysis was whether the extremes of temperature, pressure and O-ring extrusion gap would produce rupture of the O-ring material into the extrusion gap yielding "nibbling" and permanent extrusion of the rubber material.

Table 2

NOTE - All testing done on AS568-214 size O-rings		
Original Properties	AMS-7276 and MIL-R-83248C Type 1 Class 1	V75
Hardness, Shore A, ASTM D2240	75±5	78
Tensile Strength, MPa ASTM D1414	9.66 min.	13.69
Elongation, %, ASTM D1414	125 min.	205
Specific Gravity, ASTM D297	as determined	1.84
Temperature Retraction, ASTM D1329		
TR-10, degrees F	+5 or colder	+3
Air Aging ASTM D573, 70 hrs. at 518°F		
Hardness change, Shore A, ASTM D2240	-5 to +10	+2
% Tensile Strength change, ASTM D1414	-35 max.	-17
% Elongation change, ASTM D1414	-15 max.	+15
% Weight loss, ASTM D297	10 max.	3.6
Compression Set, ASTM D395 Method B and ASTM D1414, 22 hrs. at 392°F		
% Permanent set	15 max.	9.9
Compression Set, ASTM D395 Method B and ASTM D1414, 336 hrs. at 392°F		
% of Original Deflection	40 max.	28.5
ARM-200 fluid immersion, ASTM D471 and ASTM D1414, 70 hrs. at 392°F		
Hardness change, Shore A, ASTM D2240	-15 to 0	-7
% Tensile Strength change, ASTM D1414	-35 max.	-2
% Elongation change, ASTM D1414	-20 max.	+18
% Volume change, ASTM D471	+1 to +25	+16.3
Compression Set, ASTM D395 Method B and ASTM D1414, 70 hours at 392°F in ARM-200 fluid		
% Permanent set	10 max.	2.8
ASTM Fuel B immersion, ASTM D471 and ASTM D1414, 70 hrs. at 75°F		
Hardness change, Shore A, ASTM D2240	±5	-1
% Tensile Strength change, ASTM D1414	-20 max.	Nil
% Elongation change, ASTM D1414	-20 max.	+2
% Volume change, ASTM D471	0 to +5	+0.6
NOTE - International Seal, Co. (ISC) is a wholly owned subsidiary of Freudenberg-NOK.		

Table 3

NOTE - All testing done on AS568-214 size O-rings

Original Properties	AMS-R-83485 Type 1 and MIL-R-83485/1	V115
Shore A Durometer, ASTM D2240	75±5	74
Tensile Strength, MPa, ASTM D1414	11.03 min.	14.08
Ultimate Elongation, %, ASTM D1414	120 min.	196
Specific Gravity, g/cc, ASTM D297	Report	1.77
Temperature Retraction, ASTM D1329		
TR-10, degrees F	-20 max.	-22
Heat Aged, ASTM D573, 70 hrs. at 528°F		
Hardness change, Shore A, ASTM D2240	±5	-2
% Tensile Strength change, ASTM D1414	-35 max.	-19
% Elongation change, ASTM D1414	-25 max.	-5
% Weight loss, ASTM D297	-12 max.	-5.6
Compression Set, ASTM D395 Method B and ASTM D1414, Times and Temperatures as indicated		
% Permanent set, 70 hrs. at 75°F	25 max.	6
% Permanent set, 166 hrs. at 347°F	25 max.	17
% Permanent set, 22 hrs. at 392°F	20 max.	10
TT-S-735 Type III Fuel Immersion, ASTM D471 and ASTM D1414, 22 hrs. at 75°F		
Hardness change, Shore A, ASTM D2240	±5	-1
% Tensile Strength change, ASTM D1414	-30 max.	-6
% Elongation change, ASTM D1414	-20 max.	-10
% Volume change, ASTM D471	+1 to +10	+2
AMS 3021 fluid immersion, ASTM D471 and ASTM D1414, 70 hrs. at 392°F		
Hardness change, Shore A, ASTM D2240	-15 to 0	-5
% Tensile Strength change, ASTM D1414	-35 max.	-23
% Elongation change, ASTM D1414	-20 max.	-10
% Volume change, ASTM D471	+1 to +20	+14
Compression Set, ASTM D395 Method B and ASTM D1414, 70 hours at 392°F in AMS 3021 fluid		
% Permanent set	10 max.	0

NOTE - International Seal, Co. (ISC) is a wholly owned subsidiary of Freudenberg-NOK.

Table 4

Conformance to: AMS-R-25988B, Class 1, Grade 80

Note - All testing done on AS568-214 size O-rings

Original Properties	Specification	F80
Shore A Durometer, ASTM D2240	80 ± 5	80
Tensile Strength, MPa, ASTM D1414	5.17 min.	6.61
Ultimate Elongation, %, ASTM D1414	70 min.	182
Specific Gravity, ASTM D297	As determined	1.55
Air Oven Aging, ASTM D573, 70 hours at 392°F		
Hardness change, Shore A, ASTM D2240	-5 to +10	0
% Tensile Strength change, ASTM D1414	-20 max.	-12
% Elongation change, ASTM D1414	-20 max.	-11
% Weight change, ASTM D297	-2 max.	-0.2
Compression Set, ASTM D395 Method B and ASTM D1414, times and temperatures as noted		
% Permanent set, 70 hours at 75°F	20 max.	8
% Permanent set, 22 hours at 347°F	45 max.	15
AMS 3021 Fluid Immersion, ASTM D471 and ASTM D1414, 70 hours at 302°F		
Hardness change, Shore A, ASTM D2240	± 15	-8
% Tensile Strength change, ASTM D1414	-30 max.	-21
% Elongation change, ASTM D1414	-15 max.	-3
% Volume change, ASTM D471	+1 to +15	+10.7
Compression Set in AMS 3021 fluid, ASTM D395 Method B and ASTM D1414, 70 hours at 302°F		
% Permanent set	60 max.	8.1
TT-S-735 Type III Fuel Immersion, ASTM D471 and ASTM D1414, 22 hours at 75°F		
Hardness change, Shore A, ASTM D2240	-20 max.	-10
% Tensile Strength change, ASTM D1414	-30 max.	-22
% Elongation change, ASTM D1414	-30 max.	-16
% Volume change, ASTM D471	+1 to +25	+19.7
Low Temperature Retraction, ASTM D1329		
TR10, °F	-70 max.	-79

NOTE - International Seal, Co. (ISC) is a wholly owned subsidiary of Freudenberg-NOK.

Table 5

NOTE - All testing done on AS568-214 size O-rings

Original Properties	Specification	V127
Shore A Durometer, ASTM D2240	75±5	74
Tensile Strength, MPa, ASTM D1414	10.0 min.	12.9
Tensile Strength, psi, ASTM D1414	1450 min.	1875
Ultimate Elongation, %, ASTM D1414	150 min.	185
Air Aging ASTM D573, 70 hrs. at 250°C		
Hardness change, Shore A, ASTM D2240	±5	0
% Tensile Strength change, ASTM D1414	-20 max.	+5
% Elongation change, ASTM D1414	-20 max.	-8
Compression Set, ASTM D395 Method B and ASTM D1414, 22 hrs. at 200°C		
% Permanent set	20 max.	15
Mobil Jet 254 Immersion, ASTM D471 and ASTM D1414, 70 hrs. at 200°C		
Hardness change, Shore A, ASTM D2240	-10 max.	-4
% Tensile Strength change, ASTM D1414	-25 max.	-9
% Elongation change, ASTM D1414	-25 max.	-2
% Volume change, ASTM D471	0 to +5	+3.8
ASTM Fuel B Immersion, ASTM D471 and ASTM D1414, 70 hrs. at 25°C		
Hardness change, Shore A, ASTM D2240	-10 max.	-4
% Tensile Strength change, ASTM D1414	-20 max.	-13
% Elongation change, ASTM D1414	-20 max.	-2
% Volume change, ASTM D471	0 to +10	+4.0
Methanol Immersion, ASTM D471 and ASTM D1414, 70 hrs. at 25°C		
% Volume change, ASTM D471	+10 max.	+6.0
Low Temperature Glass Transition Temperature, ASTM D3418		
DSC Tg, C	-40 or colder	-42C

NOTE - International Seal, Co. (ISC) is a wholly owned subsidiary of Freudenberg-NOK.

The results for the room temperature (25°C) pressure application are shown in Figures 6-8 for the various FKM materials tested. The key to understanding Figures 6-8 is in looking at the profile of strain and comparing to the critical strain to break defined by the material property testing. If the strain observed from the FEA model approaches or exceeds the critical strain to break defined by the material property testing, then we can expect material rupture at the extrusion gap and "nibbling" of the O-ring material.

Figure 6

V75 FKM at room temperature and 6.9 MPa applied pressure
Worst case for seal
Model predicts no material rupture or “nibbling”

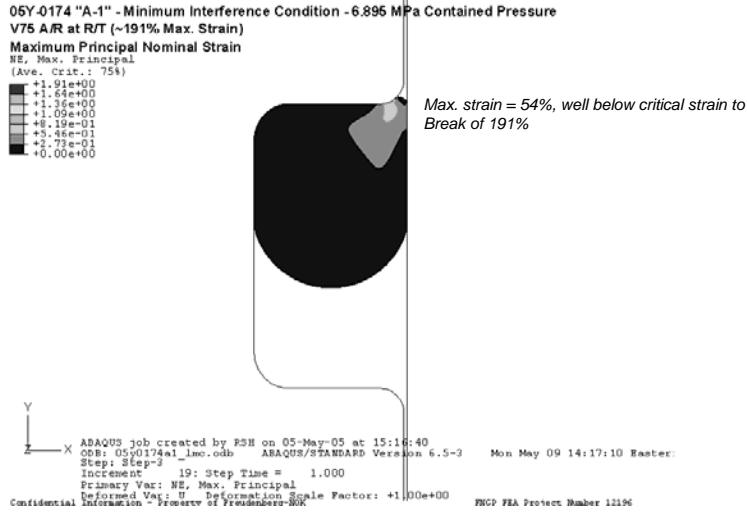


Figure 7

V115 FKM at room temperature and 6.9 MPa applied pressure
Worst case for seal
Model predicts no material rupture or “nibbling”

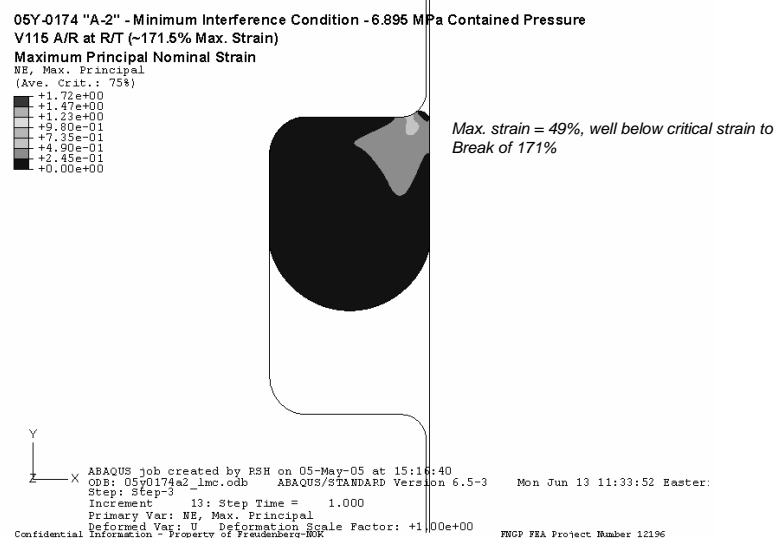
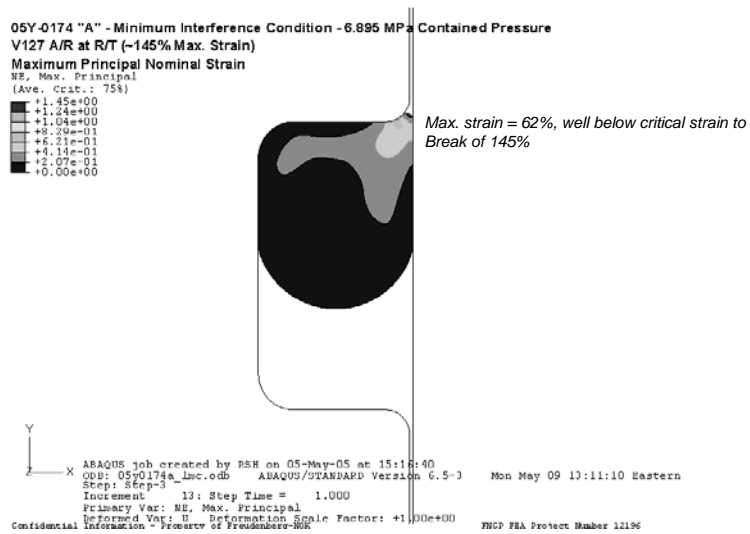


Figure 8

V127 FKM at room temperature and 6.9 MPa applied pressure
 Worst case for seal
 Model predicts no material rupture or "nibbling"



The results for the high temperature pressure application are shown in Figures 9-11 for the various FKM materials tested and in Figure 12 for the FVMQ reference material, F80. This runs contrary to the generally accepted notion that FKM's are much tougher, extrusion resistant materials than FVMQ's. The key to understanding the model predictions is in looking at the actual stress-strain curves for the various materials at the test temperatures. These curves are shown in Figures 13-17 for the materials tested. Figure 17, in particular, shows the stress-strain properties compared at 150°C - the maximum operating temperature seen by the customer.

Figure 9

V75 FKM at 150°C and 6.9 MPa applied pressure
Worst case for seal
Model predicts conditions marginal for seal material – may see “nibbling”

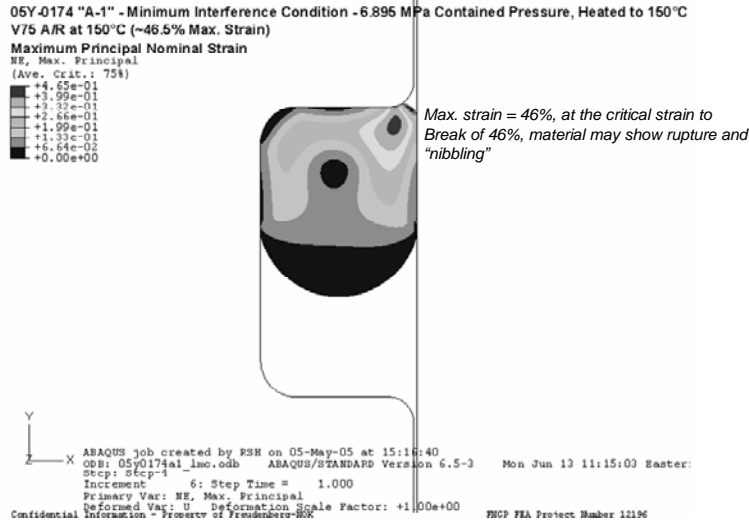


Figure 10

V115 FKM at 150°C and 6.9 MPa applied pressure
Worst case for seal
Model predicts no material rupture or “nibbling”

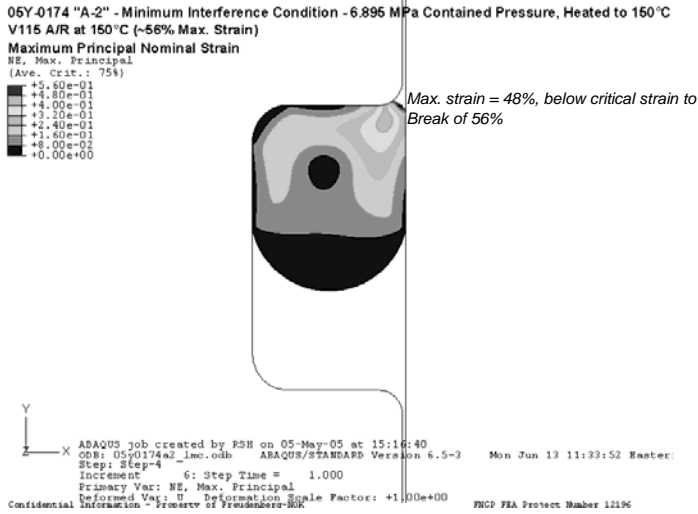


Figure 11

V127 FKM at 150°C and 6.9 MPa applied pressure
Worst case for seal
Model predicts permanent material rupture and “nibbling”

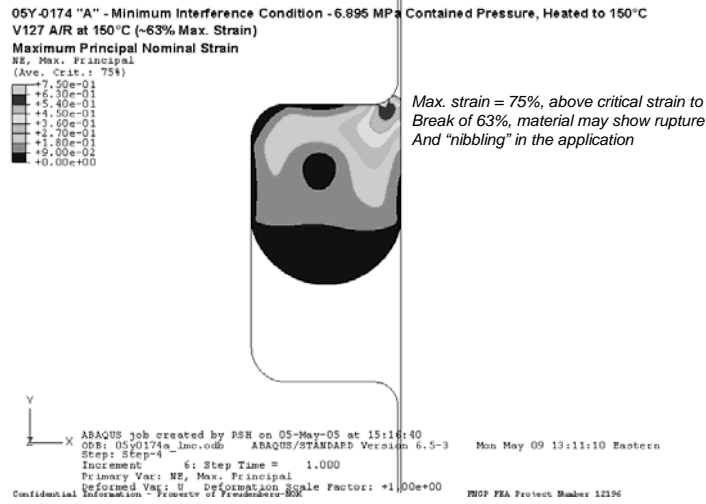


Figure 12

F80 FVMQ at 150°C and 6.9 MPa applied pressure
Worst case for seal
Model predicts no material rupture or “nibbling”

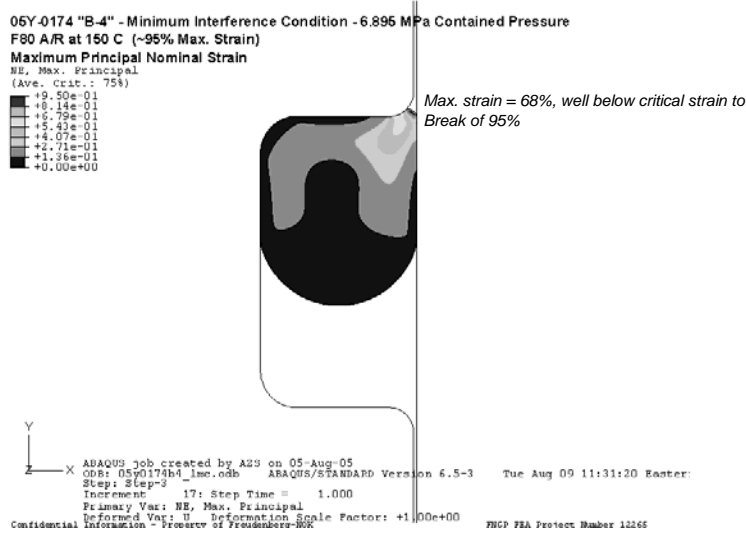


Figure 13

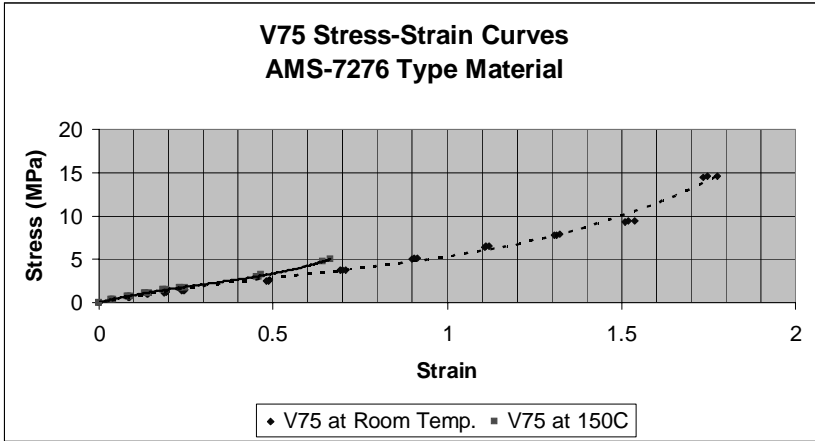


Figure 14

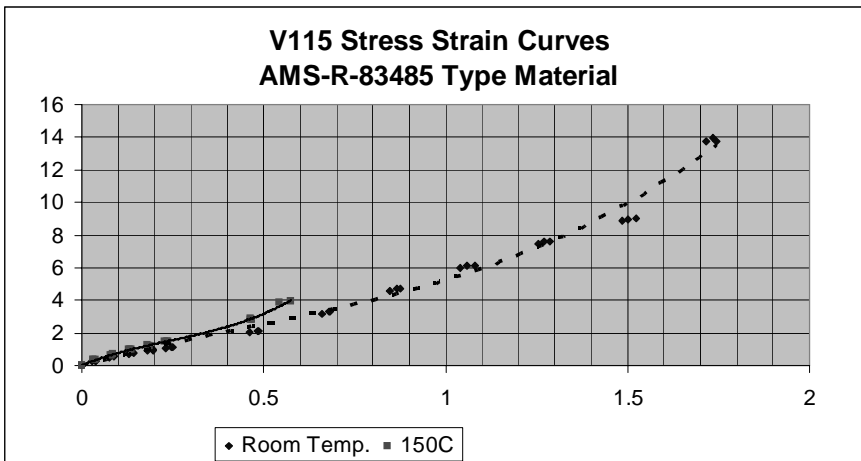


Figure 15

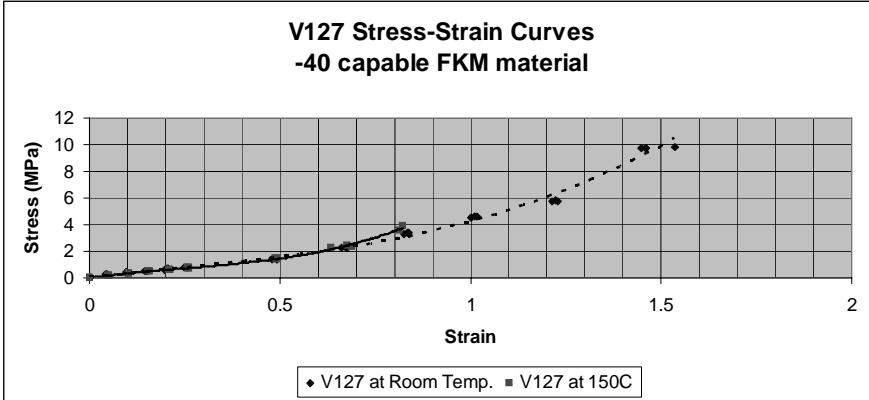


Figure 16

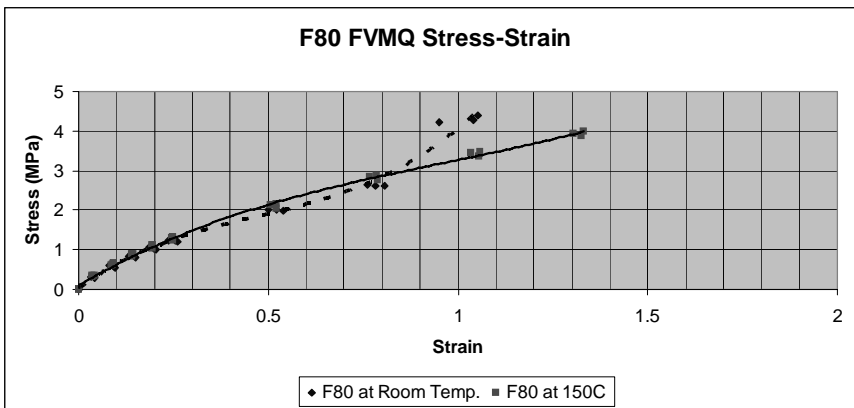
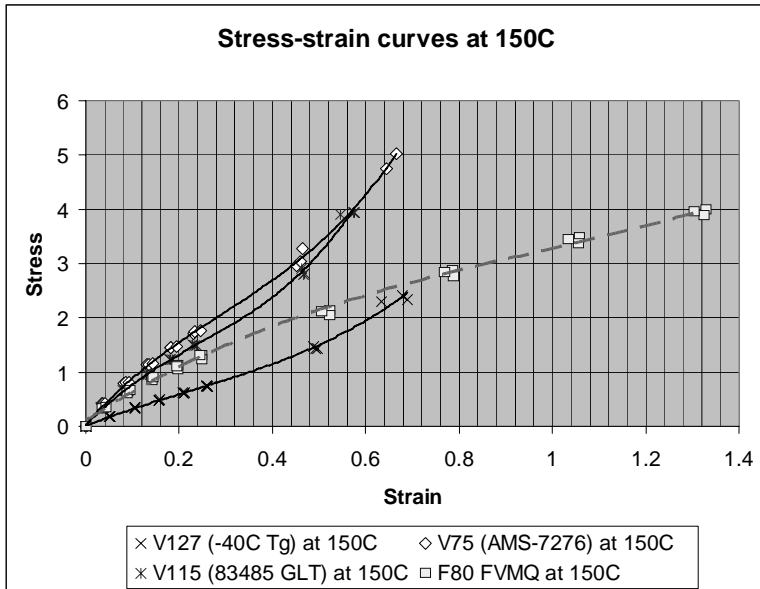


Figure 17



In each case for FKM's, the critical strain to break drops dramatically from 25°C to 150°C. The stiffness of the various FKM's remains fairly constant (initial slope of the linear portion of the stress-strain curves) going from 25°C to 150°C, but the critical strain to break (ultimate elongation) drops dramatically going from room temperature to high temperature. While this may come as a bit of a surprise, most of us who mold intricate shapes in FKM materials probably already know this since hot tear in de-molding intricate FKM parts is a major issue in our industry. Once the FKM parts cool to room temperature, they are very difficult to tear or damage.

In the case of the FVMQ material, not only does it retain its stiffness well from 25°C to 150°C, the critical strain to break of

the material is retained as well. The ability of the FVMQ material to retain its strain to break is the difference between the FVMQ material being acceptable for the high temperature, high pressure extremes of the application and the FKM materials being marginal to showing material rupture and "nibbling" in the application. The FVMQ material, F80, shows nearly twice the critical strain to break compared to any of the FKM materials tested as shown in Figure 17.

These test conditions were actually duplicated by the customer in a test rig and the results at 150°C and 6.9 MPa applied pressure showed the following results for the materials tested compared to the FEA model predictions.

Table 6

<u>Material</u>	<u>FEA model predictions at 150°C and 6.9 MPa pressure</u>	<u>Actual test rig results at 150°C and 6.9 MPa pressure</u>
FKM V75 (AMS7276, -20C Tg)	Marginal, may or may not see nibbling	No nibbling
FKM V115 (AMS-R-83485, -30C Tg)	Material OK, no nibbling predicted	No nibbling
FKM V127 (-42C Tg)	Material rupture, nibbling predicted	Nibbling observed
FVMQ F80	Material OK, no nibbling predicted	No nibbling

Noteworthy is the excellent correlation between the case of the V127 FKM where the model predicted material rupture and Nibbling and that was the observation in the test rig with the worst case for the O-ring. Likewise, the FEA model predicts no material rupture or nibbling for the F80 FVMQ material and this is what was observed in

the customer test rig. This demonstrates the utility of the material testing and FEA modeling protocol used in predicting this type of O-ring failure in pressure applications. The important point is that the material testing and FEA modeling can save money and effort since it obviates the need for the rig testing at the customer and obviates the need to build a full scale component for simulated or actual service testing, which may not be at all practical for safety critical devices on aircraft systems. So, while the material properties shown in Tables 2-5 would predict that the V127, low temperature flexible material would be superior to the FVMQ F80 material for the application, the FEA model and the actual test rig results show otherwise. The FVMQ material retains its properties at high temperature much better than any of the FKM materials tested. Conventional property testing and immersion testing would not be capable of pointing out the actual extrusion resistance of the materials in the application. The combination of conventional property and immersion testing with the FEA modeling would give a much more complete picture of the suitability of the various materials for the application.

Function Case II results - High pressure, low and high temperature aircraft phosphate ester hydraulic fluid application; effects of very minor gland design changes

In this application, the customer was interested in upgrading the seal material from an NAS-1613 Revision 2 material to an NAS-1613 Revision 5 material. The need for the upgrade was driven by

the swell of the NAS-1613 Revision 2 material in the lower density phosphate ester hydraulic fluids such as Exxon HyJet IV-A+ fluid. Fortunately, we were able to work with the customer in analyzing the design of the gland prior to any changes in the O-ring material.

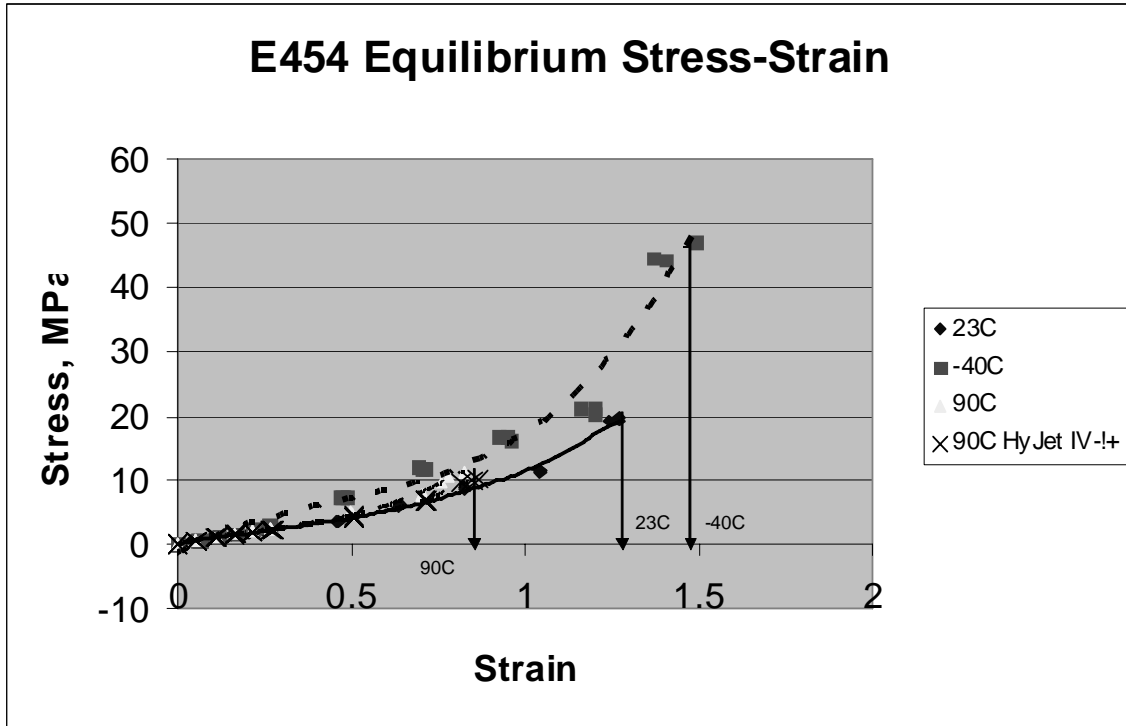
This application required the O-ring to seal without permanent extrusion rupture and "nibbling" at temperatures ranging from -40°C to $+90^{\circ}\text{C}$. The properties of the NAS-1613 Revision 5 material chosen, International Seal E454, are shown in Table 7. Actual gland extremes were obtained directly from the customer and used in the FEA analyses. The stress-strain properties at the temperature extremes for EPDM E454 are shown in Figure 18. The test conditions used to simulate the extremes of the application were:

1. -40°C
2. 23°C
3. 90°C
4. 90°C after presoaking the material in Exxon HyJet IV-A+ fluid for 24 hours at 90°C .

Table 7 - partial listing of properties, E454 EPDM to NAS-1613 Rev. 5

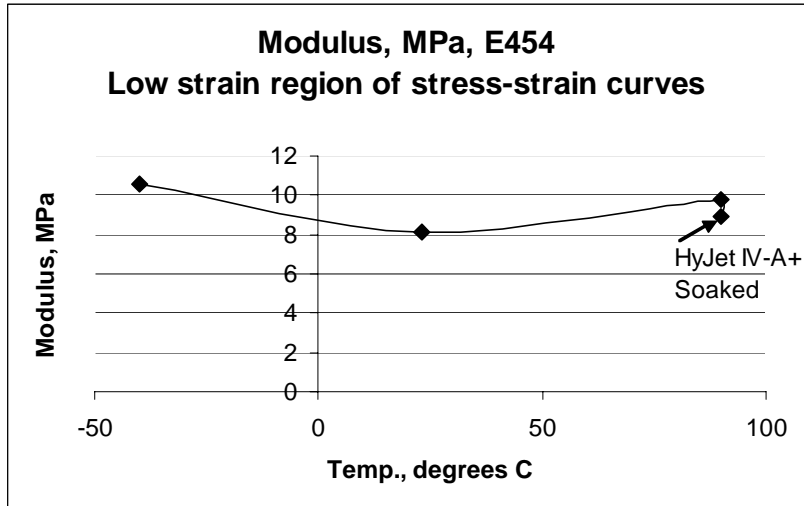
Specification: NAS 1613 Revision 5		
All testing done on AS568-214 unless otherwise noted		
Original Properties	Specification	E454
Shore A Durometer, ASTM D2240	80 ± 5	83
Tensile Strength, psi, ASTM D1414	1700 min.	2775
Ultimate Elongation, %, ASTM D1414	125 min.	151
Modulus at 100% Elongation, psi, ASTM D1414	Report	1378
Specific Gravity, ASTM D297	As determined	1.20
High Temperature Air Oven Age, ASTM D573, 70 hours at 300°F		
Hardness change, Shore A, ASTM D2240	+10 max.	+3
% Tensile Strength change, ASTM D412 Die C	-25 max.	+7.4
% Elongation change, ASTM D412 Die C	-10 max.	-1.7
Low Temperature Retraction, ASTM D1329, 75% Strain		
As Received, TR-10	-50 or colder	-67
TR-70	-18 or colder	-22
Fluid Soaked in Skydrol 500 B-4 for 70 hours at 160°F, TR-10, °F	-52 or colder	-62
Fluid Soaked in Skydrol 500 B-4 for 70 hours at 160°F, TR-70, °F	-3 or colder	-15
Fluid Soaked in Chevron HyJet IV-A+ for 70 hours at 160°F, TR-10, °F	-52 or colder	-58
Fluid Soaked in Chevron HyJet IV-A+ for 70 hours at 160°F, TR-70, °F	-3 or colder	-18
Fluid Soaked in Skydrol 5 for 70 hours at 160°F, TR-10, °F	-52 or colder	-59
Fluid Soaked in Skydrol 5 for 70 hours at 160°F, TR-70, °F	-3 or colder	-19
Compression Set, ASTM D395 Method B and ASTM D1414, AS568-330 size O-rings		
% Permanent Set, 22 hours at 250°F	30 max.	4.4
% Permanent Set, Immersed in Skydrol 500 B-4, 22 hours at 250°F	20 max.	0.8
% Permanent Set, Immersed in Chevron HyJet IV-A+, 22 hours at 250°F	20 max.	<0
% Permanent Set, Immersed in Skydrol 5, 22 hours at 250°F	20 max.	<0
% Permanent Set, Immersed in Skydrol 500 B-4, 70 hours at 160°F	20 max.	0.8
% Permanent Set, Immersed in Chevron HyJet IV-A+, 70 hours at 160°F	20 max.	0
% Permanent Set, Immersed in Skydrol 5, 22 hours at 160°F	20 max.	<0

Figure 18



As was seen with the FKM materials in Case 1, the EPDM material shows a significant drop in critical strain to break going from sub-ambient or room temperature to elevated temperature. Modulus of elasticity values were calculated for the E454 EPDM material using the slope values of the linear portions of the stress-strain curves (below 23% strain) and are shown in Figure 19. Figure 19 shows that EPDM E454 maintains a fairly constant stiffness (Modulus) across the range of temperatures and test conditions anticipated.

Figure 19



Using the stress-strain curves and the Marlow curve fitting model, the next step was simulation of the customer application at the extremes of gland and temperature. The results of the FEA analyses are shown in Figures 20-22. In the worst case of gland at the condition of +90°C after pre-soaking the material for 24 hours at +90°C in Exxon HyJet IV-A+ fluid, the FEA model predicts material rupture and “nibbling” with 24 MPa applied pressure. All other worst case gland conditions at -40° and at +23°C resulted in no predicted material rupture or “nibbling” with 24 MPa applied pressure. The question then became - would subtle changes in the gland worst case design alleviate the potential for material rupture and “nibbling?”

Figure 20

24 MPa pressure, worst case gland for seal at -40C
Model predicts no material failure or "nibbling"

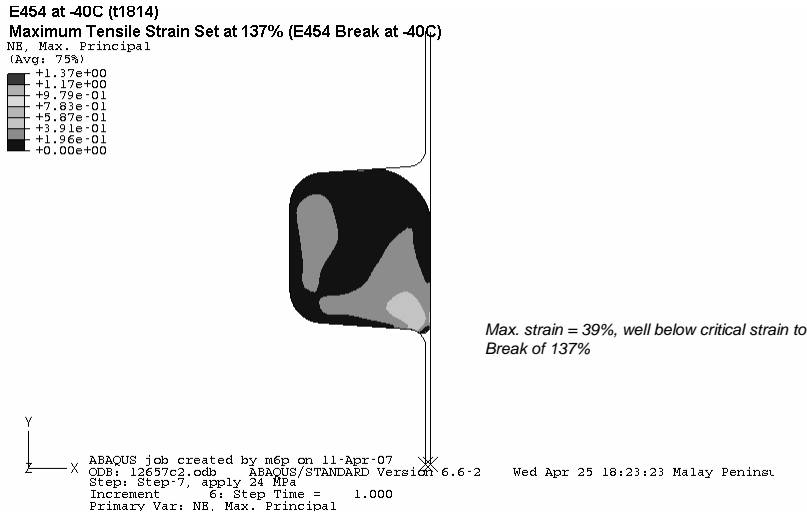


Figure 21

24 MPa pressure, worst case gland for seal at 23C
Model predicts no material failure or "nibbling"

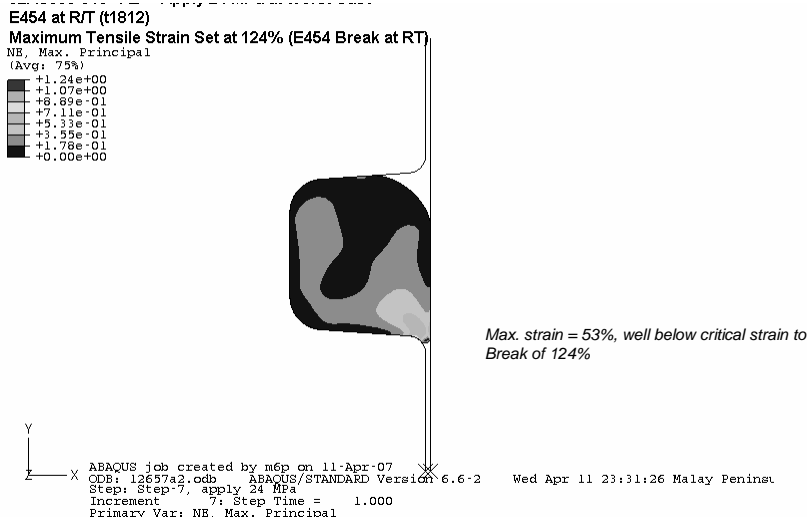


Figure 22

24 MPa pressure, worst case gland for seal at 90C after presoak in Exxon HyJet IV-A+ Model predicts material failure and “nibbling”

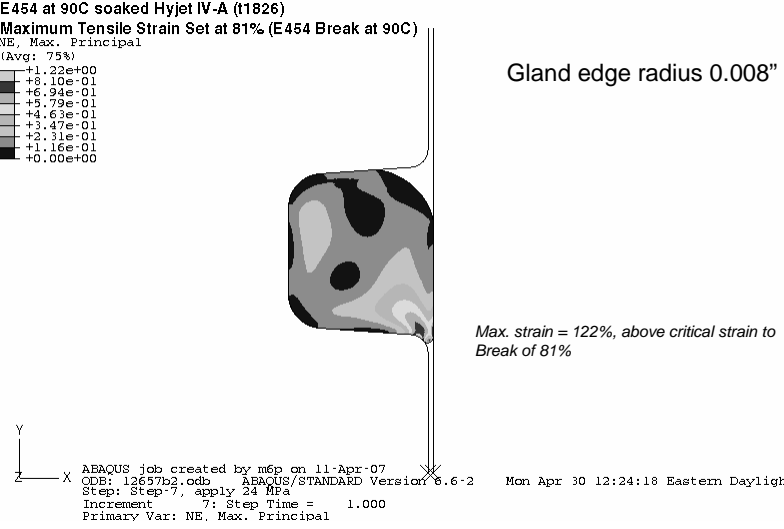


Figure 23

24 MPa pressure, worst case gland for seal at 90C after presoak in Exxon HyJet IV-A+ Model predicts no material failure or “nibbling”

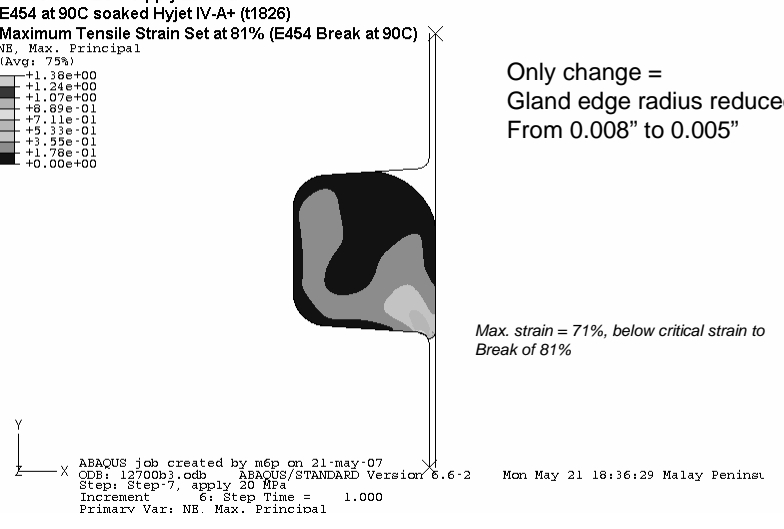
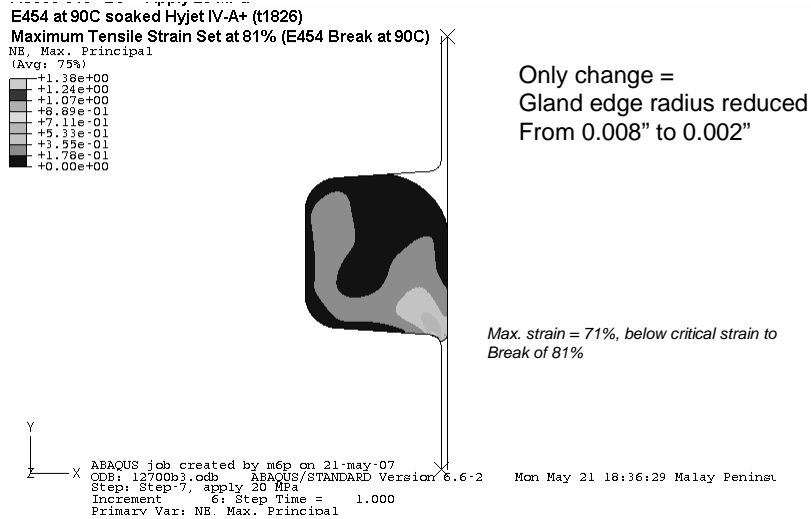


Figure 24

24 MPa pressure, worst case gland for seal at 90C after presoak
in Exxon HyJet IV-A+
Model predicts no material failure or "nibbling"



The easiest aspect of the gland worst case design to change in machining of the gland was the radius of the gland edge. The gland edge was, at worst case, a 0.008" radius. It was fairly easy in the machining process to reduce this radius from 0.008" to 0.005" or as low as 0.002" in the worst case. Figures 22-24 show the effects of reducing only the gland edge radius from 0.008" to 0.005" and down to 0.002". These are very minor and subtle changes to the gland which have a major impact on the performance of the seal as predicted by the FEA model.

We are left with the question of explaining how the very minor changes in edge radius of the gland could make such a difference in

the tendency of the material to extrude and rupture in the application. To explain this effect, it should be remembered that this can be treated like any other problem of polymer flow through a capillary⁶:

$$\sigma = (\Delta PR) / 2L \quad [7]$$

where σ = shear stress

ΔP = pressure drop through capillary

R = radius of capillary channel

L = length of capillary channel

$$\gamma = (4Q) / (\pi R^3) \quad [8]$$

where γ = shear rate

Q = volumetric flow rate of material

R = radius of capillary channel

$$\eta_{app} = \sigma / \gamma = (\Delta PR^4 \pi) / (4Q2L) \quad [9]$$

where η_{app} = apparent viscosity of material

Rearranging equation [9] to express the amount of material flow (Q):

$$Q = (\Delta PR^4 \pi) / (4\eta_{app} 2L) \quad [10]$$

Using Equation [10], we can see that very small changes in the radius of the capillary (R^4) will have huge changes on the volumetric extrusion rate of the material. Another option in this application is to increase the stiffness, or modulus, of the rubber material. In Equation [10], a term equating to modulus of the rubber is the apparent viscosity (η_{app}). We could increase the modulus of the

rubber to reduce volumetric extrusion rate of the material in the gland, but the slight reductions in gland edge radius will have a much more profound effect on reducing tendency of the material to extrude. If we assume that the apparent viscosity, or modulus, of the rubber material remains unchanged, then we can approximate the volumetric flow rate of the material through the inlet of the extrusion gap (the gland edge radius) by using Equation [10] and setting the gland edge radius to R . The pressure drop (ΔP) and the length of the extrusion gap (L) will remain unchanged and the amount of material extruding into the extrusion gap will vary by the relative volume available for rubber extrusion. If we further define the amount of material that will rupture and extrude into the extrusion gland at the original 0.008" gland edge radius as 1.00, then reducing the gland edge radius will have the following effects on reducing the amount of material that will rupture and extrude into the extrusion gap:

Table 8

Total volume of extrusion gap, Servo Valve

Entrance to extrusion gap

at 0.008" edge radius down to 0.002" edge radius

Volume available = $((0.25 * [(2R * 2R) - (\pi * R^2)]) + (R * 0.027)) * (B * \pi)$

R = groove edge radius

B = Bore diameter = 0.551"

P = worst case piston diameter = 0.54902"

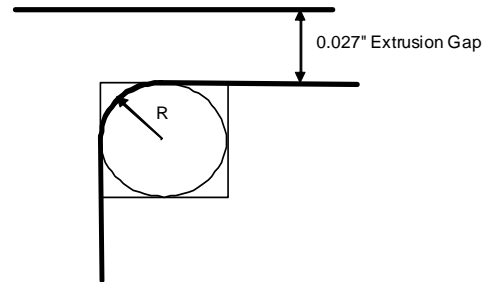
Calculation of entrance area multiplied by the Bore circumference

to get total entrance volume for extrusion

Volume at edge entrance = $Ar * \pi * P$

Q is proportional to the Volume at edge entrance

Edge radius (in)	Total Volume available for material extrusion (cu in)	<i>amount of extruded material = Q (based on volume at gap)</i>	Area of total entrance gap	Area of edge entrance (Ar), cross sectional area	<i>Volume at edge entrance</i>	<i>amount of extruded material = Q</i>
0.008	0.000398	1.000	0.02701	1.373E-05	2.369E-05	1.000
0.007	0.000345	0.868	0.02701	1.052E-05	1.814E-05	0.766
0.006	0.000294	0.739	0.02701	7.726E-06	1.333E-05	0.563
0.005	0.000243	0.611	0.02701	5.365E-06	9.254E-06	0.391
0.004	0.000193	0.485	0.02700	3.434E-06	5.922E-06	0.250
0.003	0.000144	0.361	0.02700	1.931E-06	3.331E-06	0.141
0.002	0.000095	0.239	0.02700	8.584E-07	1.481E-06	0.063



This helps illustrate the dramatic effect that gland edge radius reduction has on the tendency of the rubber O-ring material to rupture and extrude into the extrusion gap.

The use of FEA modeling, in this case, helped prove a change of material and helped demonstrate the huge effects that very subtle gland machining changes could have on the ability of the O-ring to perform without material rupture, successfully in the application. The mechanical property tests, the immersion tests, and the compression set tests of the material show that it is generally suitable for the application conditions. Without this FEA analysis, the customer may have had problems in the application only after

placing in the assembly and evaluating on the actual aircraft - a very expensive learning exercise! The use of FEA modeling along with the properties of the material helped avoid costly problems in the field by demonstrating how subtle and minor gland changes could prevent material rupture and extrusion in the application.

Conclusion and Summary

Specific cases were shown where FEA modeling predicted behavior of actual seals in the application and helped avoid costly failures in the applications. We have many more examples of the utility of FEA modeling in the development of new, broader range materials for O-ring applications. FEA modeling can be used to trouble-shoot potential application problems as well as to research potential assembly issues with O-rings and other rubber seals. The standard tests required by the industry specifications will not help in these issues and in this type of problem solving. Likewise, some of the newer tests of rubber seal durability, such as Compression Stress Relaxation, will provide no insights into these types of applications issues. Only with a thorough analysis of the material behavior along with the application conditions using FEA modeling can we accurately predict O-ring performance in the application and trouble-shoot problems - to answer the Form, Fit and Function questions.

References

- ¹ASTM Standard D2000-06, "Standard Classification System for Rubber Products in Automotive Applications," Annu. Book ASTM Stand. **09.02**, 64 (2007).
- ²Treloar, L. R. G. (1958). *The physics of rubber elasticity*. Oxford, UK: Oxford University Press.
- ³Mooney, M. (1940). *Journal of Applied Physics*, 11, 582.
- ⁴Rivlin, R. S., & Saunders, W. (1951). *Philosophical Transactions of the Royal Society, A* 243, 251.
- ⁵Bourgin, P., Cormeau, I., & Saint-Matin, J. (1995). *Journal of Material Processing Technology*, 54, 1.
- ⁶Ogden, R. W. (1972). *Proceedings of the Royal Society of London, A*(326), 525.
- ⁷White, J. L. (1978). Rheological behavior of unvulcanized rubber. In Frederick R. Eirich (Ed.), *Science and Technology of Rubber*. New York: Academic Press.